Transcriptome sequencing and metabolome analysis of food habits domestication from live prey fish to artificial diets in mandarin fish (Siniperca chuatsi)

Shan He
Huazhong Agriculture University
Jun-Jie You
Huazhong Agriculture University
Xu-Fang Liang (xfliang@mail.hzau.edu.cn)
Huazhong Agricultural University,
Zhi-Lu Zhang
Huazhong Agriculture University
Yan-Peng Zhang
Huazhong Agriculture University

Research article

Keywords: Mandarin fish, Transcriptome sequencing, Metabolome, H3K27 tri-methylation, DNA methylation, Food habits domestication

DOI: https://doi.org/10.21203/rs.3.rs-19835/v3

Abstract

Background: As economical traits, food habits domestication can reduce production cost in aquaculture. However, the molecular mechanism underlying food habits domestication has remained elusive. Mandarin fish (*Siniperca chuatsi*) only feed on live prey fish and refuse artificial diets. In the present study, we domesticated mandarin fish to feed on artificial diets. The two groups were obtained, the fish did not eat artificial diets or ate artificial diets during all of the three domestication processes, named Group W or X, respectively.

Results: Using transcriptome and metabolome analysis, we investigated the differentially expressed genes and metabolites between the two groups, and found three common pathways related to food habit domestication, including retinol metabolism, glycerolipid metabolism, and biosynthesis of unsaturated fatty acids pathways. Furthermore, the western blotting and bisulfite sequencing PCR analysis were performed. The gene expression of *TFIIF* and histone methyltransferase *ezh1* were significantly increased and decreased in the fish of Group X, respectively. The total DNA methylation levels of *TFIIF* gene and tri-methylation of histone H3 at lysine 27 (H3K27me3) were significantly higher and lower in the fish of Group X, respectively.

Conclusion: It was speculated that mandarin fish which could feed on artificial diets, might be attributed to the lower expression of *ezh1*, resulting in the decreased level of H3K27me3 and increased level of DNA methylation of *TFIIF* gene. The high expression of *TFIIF* gene might up-regulate the expression of genes in retinol metabolism, glycerolipid metabolism and glycerophosphoric metabolism pathways. Our study indicated the relationship between the methylation of DNA and histone and food habits domestication, which might be a novel molecular mechanism of food habits domestication in animals.

Background

Food habits domestication can reduce production cost in animals. Mandarin fish, as an economic species, has very unique food preference. In the wild, as soon as they start to feed, they feed exclusively on live fry of other fish species [1]. Our previous study showed transcriptome determining of food preference (dead prey fish), and indicated that retinal photosensitivity, appetite control, circadian rhythm, learning and memory outputs might be involved in the food habit domestication of dead prey fish [2]. Compared to dead prey fish, the domestication of mandarin fish to accept artificial diets can provide more profitability. However, little studies investigate the molecular regulatory mechanisms of the domestication to accept artificial diets in mandarin fish.

Previous research showed that the hormones from central nervous systems play important roles in the food intake control, such as neuropeptide Y (*NPY*) and agouti-related protein (*AgRP*) [3][4]. In giant panda, *Tas1r1* pseudogenization reinforced the herbivorous life style because of the diminished attraction of returning to meat eating in the absence of *Tas1r1* [5][6]. The ion channels polycystic kidney disease 1-like 3 (PKD1L3) and PKD2L1 linked to sour taste, and the integral membrane protein CD36 is a putative “fat taste” receptor [7]. In a leaf-eating colobine monkey, metabolism genes *pancreatic ribonuclease* gene (*RNASE1*) was contributed to its food habits (leaves) [8]. However, little is known about the genetic and metabolic regulation on the food habits domestication from live prey fish to artificial diets in mandarin fish.

It has been noted that epigenetic status might be modified by environment and diets [9]. In mice, by feeding the diets with high levels of methyl donors (e.g. folic acid) to pregnant dams, it was possible to modify the expression of the agouti gene in the offspring with the high levels of DNA methylation [10] [11]. Histone modifications correlate with transcriptional activation and repression. The maternal undernutrition led to a decreased H3K27me3 level of the promotor region and increased expression of *pomc* gene in offspring mice [12]. Therefore, whether epigenetic regulation plays an important role in the food habits domestication is unknown.

In the present study, we domesticated the mandarin fish to accept artificial diets, and conducted the transcriptome sequencing and metabolome analysis to search the common pathways of transcriptome sequencing and metabolome. In addition, using western blotting and bisulfite sequencing PCR, we examined the methylation of histone and DNA, and allowed us to gain the insights into the molecular mechanism of food habits domestication in mandarin fish, which could promote the culture of mandarin fish with artificial diets.

Results

Pathway classification map of the differentially expressed genes based on transcriptome sequencing

To obtain an overview of gene expression profile in mandarin fish of W and X groups, cDNA libraries were constructed from two groups, and sequenced using the Illumina Hiseq2000 system. High quality reads were assembled. After removing the partial overlapping sequences, a total of 77,312 distinct sequences were obtained (All-Unigene, mean size: 1,138 bp, N50: 2,334 bp). In these unigene, 49.06% (37,927) were less than 500 bp, 50.94% (39,385) were longer than 500 bp, in which 34.38% (26,578) were longer than 1000 bp. We found 54 genes to be differential expressed among the two groups, 29 and 25 genes are up-regulated and down-regulated in mandarin fish of Group X, respectively. The metabolic pathway showed the most differential expressed genes (Fig. 1A and 1B), in which lipid metabolism, signal transduction and global overview maps showed 10, 6 and 13 genes to be differentially expressed, respectively (Fig. 1A). And the rich factor of steroid biosynthesis and glycerolipid metabolism is largest of all (Fig. 1B). The details of the differential expressed genes between the two groups were presented in Table 1. The sequencing data in this study have been deposited in the Sequence Read Archive (SRA) database (accession number: PRJNA613186).

Table 1
Identification of differentially expressed gene based on transcriptome sequencing

Gene name	W Expression	X-Expression	log_2FoldChange(X/W)	KEGG map	Gene function
Phosphatidate phosphatase LPIN1	43.18282	386.1148	3.160501	Glycerolipid metabolism, Glycerophospholipid metabolism, Metabolic pathways, mTOR signaling pathway.	Generating 1,2-Diacyl-sn-glycerol
3-keto-steroid reductase-like	1.127324	20.46541	4.182214	Steroid biosynthesis, Steroid hormone biosynthesis, Metabolic pathways.	Generating 4alpha-methylzymosterol or Hydroxyestrone
general transcription factor IIF subunit 2 isoform X2	1.302917	25.49286	4.290276	Basal transcription factors.	Transcription
sterol-4alpha-carboxylate 3-dehydrogenase	10.80255	140.7436	3.703626	Steroid biosynthesis, Metabolic pathways.	Generating 3-Keto-4-methylzymosterol
endothelial lipase	72.61555	753.4305	3.375124	Glycerolipid metabolism, Metabolic pathways.	Generating fatty acid
serum/glucocorticoid-regulated kinase 1	1.328233	33.50641	4.656857	mRNA surveillance pathway, cAMP signaling pathway, cGMP-PKG signaling pathway, Oocyte meiosis, Adrenergic signaling in cardiomyocytes, Vascular smooth muscle contraction, Hippo signaling pathway, Focal adhesion, Platelet activation, Long-term potentiation, Dopaminergic synapse, Inflammatory mediator regulation of TRP channels, Regulation of actin cytoskeleton, Insulin signaling pathway, Oxytocin signaling pathway.	
ATP-binding cassette, subfamily C (CFTR/MRP), member 12	1.067294	25.75915	4.593055	ABC transporters.	
stearoyl-CoA desaturase	863.601	10415.86	3.592273	Biosynthesis of unsaturated fatty acids, Fatty acid metabolism, PPAR signaling pathway, AMPK signaling pathway, Longevity regulating pathway – worm.	Fatty acid desaturation
PH domain and leucine-rich repeat-containing protein phosphatase	4.106606	53.87121	3.713496	hospholipase D signaling pathway, Neuroactive ligand-receptor interaction, Glutamatergic synapse	
Retinol dehydrogenase 12	7.270524	99.28454	3.771438	Retinol metabolism, Metabolic pathways	Generating all-trans-Retinal
lymphokine-activated killer T-cell-originated protein kinase homolog	6.070951	145.7947	4.585872	Pancreatic secretion, Protein digestion and absorption	
5-phosphohydroxy-L-lysine phospho-lyase	1.974891	34.93728	4.144922	Lysine degradation, Metabolic pathways	Generating Allysine
transcription factor CP2-like protein 1	33.3349	1.088583	-4.93651		
serum/glucocorticoid regulated kinase 1	87.45664	1.841215	-5.56984	FoxO signaling pathway, mTOR signaling pathway, PI3K-Akt signaling pathway, Aldosterone-regulated sodium reabsorption	
hypoxia up-regulated 1	135.8593	1.88101	-6.17446	Protein processing in endoplasmic reticulum	
Alcohol dehydrogenase [NADP(+)] A	550.9179	101.9587	-2.43385	Glycolysis / Gluconeogenesis, Pentose and glucuronate interconversions, Glycerolipid metabolism, Metabolic pathways	Generating glucuronate, ethanal or D-Glyceraldehyde
Phosphatidate phosphatase LPIN1	230.0628	21.91613	-3.39196	Glycerolipid metabolism, Glycerophospholipid metabolism, Metabolic pathways, mTOR signaling pathway	
Copper-transporting ATPase 2	923.8284	210.7988	-2.13176	Mineral absorption	

False Discovery Rate (FDR) ≤ 0.001, Fold Change ≥ 1.00

Gene name	W Expression	X-Expression	log_2FoldChange(X/W)	KEGG map	Gene function
calcium/calmodulin-dependent serine protein kinase	55.2038	1.86159	-4.89016	Tight junction	
solute carrier family 2, facilitated glucose transporter member 5	16.81712	0.94255	-4.15722	Carbohydrate digestion and absorption	Froctose or glucose absorption
phosphoglycolate phosphatase	15.43525	0.934372	-4.04609	Glyoxylate and dicarboxylate metabolism, Metabolic pathways, Carbon metabolism	Generating glycolate
Nuclear receptor coactivator 7	31.91563	1.559127	-4.35545	RNA degradation	
Plasma kallikrein	20520.24	418.6751	-5.61507	Complement and coagulation cascades	
complement component 2	2119.225	73.06701	-4.85817	Complement and coagulation cascades,	
False Discovery Rate (FDR) ≤ 0.001, Fold Change ≥ 1.00					

Analysis of differential metabolites of two Groups.

The metabolic profiles of plasma samples from the two groups were analyzed by LC-MS in positive (ESI+) and negative (ESI−) scan modes. In total, 9,249 iron number were selected in the final data table for subsequent analyses (4,155 iron number in ESI+ mode and 5,094 iron number in ESI− mode).

The acquired normalized data were analyzed by PCA and PLS-DA using multivariate analysis. The PCA score plot showed two clusters of data obtained from different groups in positive and negative ion scan modes (Fig. 2A). The two groups were separated clearly in the score plot by the first two components. To obtain better discrimination between the groups, PLS-DA was performed. A clear separation of Group W and X showed in Fig 2B, which suggested that significant biochemical changes existed between the two groups. The results based on hierarchical clustering analysis (HCA) of the differential metabolites indicated that Group X and W showed significant difference (Fig. 2C). The information of these metabolomic biomarkers was listed in Table 3.

Potential metabolom

VIP		1.412466	1.412466	1.412466	1.938388	1.148462679	1.505221	1.505221	1.505
Fragmentation score		0.344	0	0	35.4	0	5.95	0	5.95
Score		37.7	37.6	36.6	45.1	27.4	38.8	35.9	38.8
m/z		190.0466	190.0466	190.0466	475.2051	259.1044545	307.2013	307.2013	307.2
RT(min)		3.577217	3.577217	3.577217	7.691483	7.78	7.808933	7.808933	7.808
Metabolites	ESI+	Isopyridoxal;	Pyridoxal;	sn-Glycerol 3-phosphate	5,10-Methylenetetrahydrofolate	5-Amino-6-(1-D-ribitylamino)uracil	L-Hyoscyamine	11-cis-Retinal	Littor

To identify the metabolites, a database search was further performed using the freely accessible database of Kyoto Encyclopedia of Genes and Genomes (KEGG) to elucidate the putative function of the metabolites. 44 and 20 irons were identified by MS1 and MS2 level in positive mode respectively, and 24 and 11 irons in MS1 and MS2 level in negative mode respectively. The details of differential ions between the two groups were presented in Table 2.

Table 2
Identification of differential ions based on metabolome

Differential ions					Metabolites identification					
Comparison among groups	Detect mode	Total ion number	Up-regulated	Down-regulated	MS1 ions number			MS2 ions number		
					Total	Up-regulated	Down-regulated	Total	Up-regulated	Down-regulated
X vs W	Positive	127	86	41	44	32	12	20	16	4
	Negative	116	65	51	24	17	7	11	7	4
The number of all of the differential m/z between the two groups, which including identified ions and unable identified ions.										
MS: the number of identified ions by searching KEGG database associated with primary data (parent ions).										
MS2: the number of identified ions by searching fragmentation information available from KEGG database.										

The common pathways of differential metabolites and genes.

In retinol metabolism pathway, retinol, 9-cis-retinol and 11-cis-retinol metabolites were higher in mandarin fish of Group X than those of Group W, RDH (retinol dehydrogenase) gene expression was consistently higher in Group X (Fig. 3A). In glycerolipid metabolism pathway, triacylglycerol lipase gene expression was higher in mandarin fish of Group X, and glycerophosphoric metabolites was also higher in Group X (Fig. 3B). In biosynthesis of unsaturated fatty acids pathway, stearoyl-CoA gene expression and DPA (docosapentaenoic acid) metabolites were higher in fish of Group X than those in Group W (Fig. 3C).

***TFIIF* gene expression and DNA methylation.**

As is shown in Fig 4A, *General transcription factor IIF* (*TFIIF*) gene expression was higher in the mandarin fish of Group X than that of Group W. We then analyzed the CpG islands at −5000 bp upstream from the transcription initiation site (designated as 0) of *TFIIF* by methylation analysis software. As shown in Fig.4B, one CpG islands containing 9 CpG sites existed in −3619 to −3574 bp of *TFIIF* gene. The total DNA methylation level was significantly higher in the fish of Group X than that of Group W (Table 4).

Table 4
Methylation of each CpG island of *TFIIF* gene betwe

VIP	1.777018	1.623949	2.568626	2.246171	2.568625927	2.663185	2.132225	2.29817
Fragmentation score	0	95.1	0	88.4	92.4	0	0	31.9
Score	37.4	57.9	37.6	56.1	56.1	33.4	37	43.6
m/z	271.0812	203.0818	303.2325	243.0614	303.2325012	627.2114	289.0671	313.237
RT(min)	5.166667	3.5915	7.391183	1.374833	7.391183333	8.206233	1.395567	7.19901
Metabolites	D-Lombricine ESI-	L-Tryptophan	Arachidonate	Uridine	Taxa-4(20),11(12)-dien5alpha,13alpha-diol	Chlorophyllide b	Galactosylglycerol	(12Z)-9, Dihydro 12-enoic

***Ezh1* gene expression and histone methylation**

The mRNA expression of histone methyltransferase *ezh1* gene was lower in the mandarin fish of Group X (Fig. 5A). As histone methyltransferase Ezh1 could methylate 'Lys-27' of histone H3, we analyzed the H3K27me3 levels of the two groups. The results showed that H3K27me3 level was also lower in the mandarin fish of Group X than that of Group W (Fig. 5B).

Discussion

In rearing conditions, mandarin fish accept only live prey fish, refusing dead prey fish or artificial diets [13]. Although pervious research showed the methods of mandarin fish domestication [14], little is known about the mechanism of food habits domestication. In the present study, we domesticated the mandarin fish to feed on artificial diets, and found a part of mandarin fish could accept artificial diets easily (Group X), but another part could not accept completely (Group W). To uncover the molecular mechanism why mandarin fish refuses artificial diets, we conducted the transcriptome sequencing and metabolome analysis. The results showed that the differentially expressed gene between the two groups were enriched in metabolism, in which the global and overview maps and lipid metabolism were the most enriched. And the rich factors of steroid biosynthesis and glycerolipid metabolism were the highest. The metabolome results showed that the pathways with different metabolites were mostly enriched in the metabolic pathways, which were consistent with transcriptome sequencing results. Previous research has shown that the most important pathways related to the domestication of dead prey fish in mandarin fish included the retinal photosensitivity, circadian rhythm, appetite control, learning and memory pathway [2]. Our results showed that metabolism, especially lipid metabolism, might contribute to the domestication of artificial diets, which was different from the domestication of dead prey fish, as the different constituents between dead prey fish and artificial diets.

We then analyzed the pathways in which the differential genes or metabolites were involved, the common pathways which showed the most enriched differential genes and metabolites, were retinol metabolism, glycerolipid metabolism and biosynthesis of unsaturated fatty acids. For retinol metabolism, retinol, 9-cis-retinol and 11-cis-retinol metabolites were higher in the Group X, consistently the *RDH* (*retinoldehydrogenase*) gene expression was higher in the Group X, suggesting a better visual acuity in the mandarin fish which could be easy to accept artificial diets. Animals make food choices based on the physiological, nutritional, environmental, and sociocultural factors [15], sensory system is of significance to food choices. It is critical for mandarin fish to catch prey fish though the perception of shape and motion with well-developed scotopic vision [16]. *Salmo spp.* shows the same motion and shape of food and the offered food pellet can be captured immediately before it falls down to the bottom of the tank because they have high visual acuity, thus can feed swiftly by darting [17][18][19]. But mandarin fish has low visual acuity and feed only by stalking, it can not recognize the prey before the time when food pellet fall to the bottom of tank, thus makes it difficult to feed mandarin fish with artificial diets [20]. The retinol metabolism dysfunction might be contributed to the lower visual ability in the mandarin fish which refused artificial diets.

In glycerolipid metabolism pathway, the gene expression of triacylglycerol lipase was higher in the mandarin fish of Group X, and the glycerophosphoric acid metabolite was also higher in the Group X. In the biosynthesis of unsaturated fatty acids pathway, stearoyl-CoA gene expression and docosapentaenoic acid

(DPA) metabolite were higher in the Group X. These results suggested that mandarin fish which could accept artificial diets well, might be attributed to the better capacity of glycerolipid metabolism and unsaturated fatty acids biosynthesis. Live food diets (such as zooplankton) and dry formulated diets have different fat levels and influences in European grayling [21]. Artificial diets might have more fat and energy than live prey fish, suggesting that mandarin fish which accept artificial diets could make good use of fat, while the fish which refuse artificial diets could not.

To elucidate the regulatory mechanism of up-regulated gene expression in the mandarin fish of Group X, we analyzed the differentially expressed genes based on transcriptome sequencing. The results showed *TFIIF* gene expression was significantly increased in the Group X. TFIIF communicates with a number of factors to regulate gene transcription. It has been reported that TFIIF directly binds to basal factors of TFIID, TFIIE and TFIIB [22]. TFIIF has been shown to be necessary for most, if not all, preinitiation complex formation and gene transcription [23][24]. It suggested that in the mandarin fish which accepted artificial diets, the up-regulated transcription of genes, involved in retinol metabolism, glycerolipid metabolism and biosynthesis of unsaturated fatty acids, might be contributed to the increased *TFIIF* expression.

To uncover why *TFIIF* was upregulated in the mandarin fish of Group X, the expressions of histone methyltransferases were analyzed based on transcriptome. The expression of histone-lysine N-methyltransferase *ezh1* was significantly decreased in the Group X. Histone methyltransferases EZH1 and EZH2 catalyze the tri-methylation of H3K27, which serves as an epigenetic signal for chromatin condensation and transcriptional repression [25]. In mice, Ezh1 was required for neonatal heart regeneration after myocardial infarction and overexpression of Ezh1 promoted heart regeneration by upregulating cardiac muscle growth genes [26]. Furthermore, we observed the protein level of tri-methylation of histone H3 at lysine 27 was lower in the Group X, suggesting an active function of gene expression. The decreased abundance of histone H3K27me3 was also found in *FOXO1* (*forkhead box protein O1*) in HFD (high fat diets) fed rats, which persisted even after 8 weeks of diet reversal [27]. In addition, the total DNA methylation level of *TFIIF* was significantly higher in the mandarin fish of Group X than those of Group W. The mRNA level of *TFIIF* was higher in fish of Group X, our results showed a positive effect of DNA methylation on gene expression. In soybean, the genome-wide methylation profiles showed that hyper-methylated genes had higher gene expression[28], in ventricular septal defect patients, genome-wide DNA methylation data showed 12 hypermethylated genes had a higher gene expression[29]. In Arabidopsis, upon loss of CpG methylation, there was target-specific enrichment of H3K27me3 in heterochromatin that correlated with transcriptional reactivation, it is suggested that there was an antagonistic effect between CpG methylation and H3K27me3 [30]. It is hypothesized that the lower *ezh1* expression in the mandarin fish of Group X, could be contributed to the decreased methylation at 'Lys-27' of histone H3, and then up-regulating the expression and methylation of *TFIIF* gene.

Conclusions

Our research indicated the individual differences of acceptance on artificial diets in mandarin fish and the potential molecular mechanism. The mandarin fish which feed on artificial diets, could down-regulate the *ezh1* expression, repressing the tri-methylation level of histone H3 at lysine 27, and then resulting in the increased DNA methylation and mRNA expression of *TFIIF* gene. TFIIF as an important transcription factor, might regulate the expression of genes involved in retinol metabolism, glycerolipid metabolism and glycerophosphoric metabolism, and modify the acceptance on artificial diets of mandarin fish. These results suggested the potential effect of histone methylation on food habits domestication in mandarin fish.

Methods

Fish domestication and sampling

Mandarin fish were obtained from Chinese Perch Research Center of Huazhong Agricultural University (Wuhan, Hubei Province, China). Fish (50 ± 5 g) were maintained in the aquarium (12 tanks, 50 fish per tank) with continuous system of water filtration and aeration at constant temperature (25 ± 0.5 °C) and domesticated. Mandarin fish were fed with artificial diets (Table 6) and divided into two groups: fish did not eat artificial diets and fish ate artificial diets. The fish did not eat artificial diets during the first domestication process was then fed with live fish prey for three days, starved for two days and fed with artificial diets for one day, and then we selected the fish did not eat artificial diets during the second domestication process and repeated the domestication process for one more time. The fish ate artificial diets during the first domestication process was fed with live fish prey for one days and fed with artificial diets for three days, then we selected the fish ate artificial diets during the second domestication process and repeated the domestication process for one more time. Finally, the two groups were obtained, the fish did not eat artificial diets or ate artificial diets during all of the three domestication processes, named Group W (n=42) or X (n=24), respectively. Six fish were used for real-time quantitative PCR. Six fish were used for western blotting. Ten fish were used for metabolome**,** and three fish were used for transcriptome sequencing.

Table 6
Composition of artificial diets

Primers for real-time PCR	Sequences(5'-3')
RPL13A-F	CACCCTATGACAAGAGGAAGC
RPL13A-R	TGTGCCAGACGCCCAAG
EZH1-F	AAAAGATTGAGCAGCAGACA
EZH1-R	GGAAGCCAAACTCCACTGTA
TFIIF-F	GTGCCCAAATACCTCTCTCAGC TCTATACCCTCAATCACAGTCAGC
TFIIF-R	
Primers for BSP amplicon	Sequences(5'-3')
BSP *TFIIF*-F	TTTAGGGTTTTGATTTTGGTTTTTT
BSP *TFIIF*-R	ACTAAATAAACAACTCTTCATTTTAC
Ingredients	**%**
White fish meal	71
Corn starch	8
Fish oil	10
Vitamin premix[1]	2
Mineral premix[2]	2
Microcrystalline cellulose	2
Carboxymethyl cellulose	2
Yeast extract powder	3
Note: 1. Vitamin premix (per kg of diet): vitamin B1 (thiamin), 30 mg; vitamin B2 (riboflavin), 60 mg; vitamin B6, 30 mg; vitamin B12, 0.22 mg; vitamin D3, 5 mg; vitamin E 160 mg; vitamin K3 50 mg; folic acid, 20 mg; biotin, 2.5 mg; pantothenic acid calcium, 100 mg; ascorbic acid (35%), 250 mg; niacinamide, 200 mg; powdered rice hulls, 999 mg.	
2. Mineral premix (per kg of diet): MnSO4, 10 mg; MgSO4, 10 mg; KCl, 95 mg; NaCl, 165 mg; ZnSO4, 20 mg; KI, 1 mg; CuSO4, 12.5 mg; FeSO4, 105 mg; Na2SeO3, 0.1 mg; Co, 1.5 mg.	

The experimental fish were anesthetized with MS-222 (200 mg/L) (Redmond, WA, USA) and sacrificed by decapitation according to the ethical guidelines of Huazhong Agricultural University. Immediately after the surgical resection, the liver tissue was frozen in liquid nitrogen and stored at -80 °C until used. The blood was drawn from the tail vein. The whole blood sample was separated with 4000 r/centrifuge for 10 min, collecting plasma and storing at -80 °C. The animal protocol was approved by the Institutional Animal Care and Use Ethics Committee of Huazhong Agricultural University (Wuhan, China) (HZAUFI-2017-015).

RNA Isolation and Reverse Transcription

Total RNA was extracted and one microgram of total RNA was synthesized to complementary DNA (cDNA) using Trizol reagent and Revert Aid™ Reverse Transcriptase (TaKaRa, Tokyo, Japan) following the manufacturer's instructions, respectively.

Transcriptome Sequencing

Equal amount of total RNA from each group (n=3) were used to construct the libraries for transcriptome analysis using MGIEasy RNA kit following manufacturer's instructions (BGI, Wuhan, China). Paired-end cDNA libraries were sequenced using BGISEQ-500 system (BGI, Wuhan, China). Image deconvolution, base calling, unigene assembly, annotation and expression level estimation were carried out as described by You et al [31]. We analyzed the differentially expressed genes used DEGseq method described before [32], and False Discovery Rate (FDR) ≤ 0.001 and Fold Change ≥ 2.00 as the threshold to judge the significance of gene expression difference. GO function and KEGG pathway analysis were then carried out in the differentially expressed genes.

Metabolome

Serum samples (40 μl, including QC samples) were added to new Eppendorf tubes with ice-cold methanol (120 μl), vortex mixed for 1min, placed in holding for 30min at -20 °C, and centrifuged at 4000 g for 20 min at 4 °C. 25 μl of supernatant and 225 μl 50% methanol were mixed. Then 20 μl of mixture from each sample were mixed as quality control samples, 60 μl of mixture was conducted as samples. All samples were stored at -80 °C (ten biological replicates for each group).

All samples were acquired by the LC-MS system followed machine orders. Chromatographic separations were performed using an ultra performance liquid chromatography (UPLC) system (Waters, USA) and a high-resolution tandem mass spectrometer SYNAPT G2 XS QTOF (Waters, USA) was used to detect metabolites as the methods described by Huang et al [33]. The mass spectrometry data were acquired in Centroid MSE mode. Statistical analysis was performed as previous [34]. Putative metabolites were first derived by searching the exact molecular mass data from redundant m/z peaks against the online HMDB (http://www.hmdb.ca/), METLIN (http://metlin.scripps.edu/) and KEGG (www.genome.jp/kegg/) databases.

Real-time Quantitative PCR

Primers were designed with Primer 5.0 software based on the sequences which was obtained from transcriptome sequencing data of mandarin fish, and synthesized by Sangon (Shanghai, China) (Table 5). Several housekeeping gene including *beta-actin*, *b2m*, *rpl13a*, and *hmbs* were selected according to the literature [35]. *Rpl13a* gene was more stable and amplified as the internal control. Real-time quantitative PCR was carried out with MyiQ™ 2 Two-Color Real-Time PCR Detection System (Bio-Rad, Hercules, USA) as the methods described by Liang et al [36]. Gene expression levels were quantified relative to the expression of *rpl13a* using the optimized comparative Ct ($2^{-\Delta\Delta Ct}$) value method [37]. Data were presented as mean ± S.E.M with six biological replicates and three technical replicates.

Table 5
Nucleotide sequences of the primers

CpG Position	-3696	-3689	-3686	-3647	-3645	-3627	-3605	-3601	-3524	total
ME-CPG	9/30	21/30	21/30	22/30	22/30	22/30	21/30	22/30	0/0	170/236 72.0%
X	63.3%	70.0%	70.0%	73.3%	73.3%	73.3%	70.0%	84.6%	0.0%	
ME-CPG	15/30 50.0%	18/30	17/30	19/30	17/30	18/30	19/30	19/29	0/13	142/252 56.3%
W		60.0%	56.7%	63.3%	56.7%	60.0%	63.3%	65.5%	0.0%	
significance	0.114	0.417	0.284	0.405	0.176	0.273	0.584	0.105	\	0.000*

DNA methylation analysis

Genomic DNA was extracted following the standard procedures using TIANamp Genomic DNA Kit (Tiangen, Beijing, China). DNA treatment with sodium bisulfite was performed using the EZ DNA Methylation Kit (Zymo Research, USA) according to the manufacturer's protocol. The BSP primers were designed by the online MethPrimer software 14 and Primer 5.0 (Table 5). PCR products were subcloned and sequenced as the methods described by Cai et al [38]. Six samples from the mandarin fish of Group W or X were analyzed with five technical replicates.

Western Blotting

Liver tissue stored at -80 °C were solubilized in lysis buffer, and lysates were separated on 10% SDS-PAGE gel. Proteins were then transferred onto PVDF membrane. Tri-Methyl-Histone H3 (lys27) (C36B11) Rabbit mAb was obtained from Cell Signaling Technology (Danvers, MA). The protein level H3K27me3 were detected by western blotting with the antibody (1:1000-1:4000) according to manufacturer's instructions. Blots were probed by second antibody with IR-Dye 680 or 800 cw labeled (1:2000-1:4000, Licor, Lincoln, NE, USA) and the membranes were visualized and quantified as the methods described by You et al [31]. (six biological replicates for each group).

Statistical Analysis

Statistical analyses were conducted with SPSS 19.0 software. All data were tested for normality and homogeneity of variances using the Shapiro-Wilk's test and Levene's test, respectively. One-way analysis of variance (ANOVA) were using to find significant differences, followed by Duncan's multiple range tests and Fisher's least significant difference post hoc test, after confirming data normality and homogeneity of variances. Differences were considered to be significant if $P < 0.05$.

Abbreviations

EZH1: histone H3-lysine27 N-trimethyltransferase EZH1; H3K27me3: histone H3-lysine27 tri-methylation; TFIIF: general transcription factor IIF; NPY: neuropeptide Y; AgRP: agouti-related protein; Tas1r1: taste receptor type 1 member 1; PKD1L3: polycystic kidney disease 1-like 3; PKD2L1: polycystic kidney disease 2-like 1; RNASE1: pancreatic ribonuclease; B2m: beta-2-microglobulin; Rpl13a: ribosomal protein L13a; Hmbs: hydroxymethylbilane synthase; QC: Quality control; PCA: principal component analysis; LC-MS: liquid chromatography mass spectrometry; KEGG: Kyoto Encyclopedia of Genes and Genomes, RDH: retinol dehydrogenase; DPA: docosapentaenoic acid; GO: Gene Ontology; FOXO1: forkhead box protein O1; HFD: high fat diets; UPLC: ultra performance liquid chromatography; FDR: False Discovery Rate; ANOVA: One-way analysis of variance.

Declarations

Ethics approval and consent to participate

The animal protocol was approved by the Institutional Animal Care and Use Ethics Committee of Huazhong Agricultural University (Wuhan, China) (HZAUFI-2017-015).

Consent to publish

Not applicable.

Availability of data and materials

The sequencing data in this study have been deposited in the Sequence Read Archive (SRA) database (accession number: PRJNA613186).

Competing interests

The authors declare that they have no conflict of interest.

Funding

This work was financially supported by the China Agriculture Research System (CARS-46), Wuhan Morning Light Plan of Youth Science and Technology (No. 2017050304010318), and the National Natural Science Foundation of China (31772822).

Author Contributions

S.H., J.J.Y., Z.L.Z. and Y.P.Z. contributed to the sample preparation and examination. S.H. and L.L. performed the assembly and bioinformatical analysis. S.H. and J.J.Y. performed the data analysis. S.H. and X.F.L. gave technical advice and contributed to the study design. S.H. and J.J.Y. wrote the paper. All authors read and approved the final manuscript.

Acknowledgments

Not applicable.

References

1. Liang XF, Lin X, Li S, Liu JK. Impact of environmental and innate factors on the food habit of Chinese perch *Siniperca chuatsi* (Basilewsky) (Percichthyidae). Aquac. Res. 2008;39:150-157.
2. He S, Liang XF, Sun J, Li L, Yu Y, HuangW, Qu CM, Cao L, Bai XL, Tao YX. Insights into food preference in hybrid f1 of *siniperca chuatsi* (♀) × *siniperca scherzeri* (♂) mandarin fish through transcriptome analysis. BMC Genomics. 2013;14.
3. Morton GJ, Cummings DE, Baskin DG, Barsh GS, Schwartz MW. Central nervous system control of food intake and body weight. Nature, 2006;443:289-295.
4. Cone RD: Anatomy and regulation of the central melanocortin system. Nat Neurosci.2005;8:571-578.
5. Zhao H, Yang JR, Xu H, Zhang J: Pseudogenization of the umami taste receptor gene Tas1r1 in the giant panda coincided with its dietary switch to bamboo. Mol Biol Evol. 2010;27:2669-2673.
6. Li R, Fan W, Tian G, Zhu H, He L, Cai J, Huang Q, Cai Q, Li B, Bai Y, et al. The sequence and de novo assembly of the giant panda genome. Nature.2010;463:311-317.
7. Garcia-Bailo B, Toguri C, Eny KM, El-Sohemy A. Genetic variation in taste and its influence on food selection. OMICS. 2009;13:69-80.
8. Zhang J, Zhang YP, Rosenberg HF. Adaptive evolution of a duplicated pancreatic ribonuclease gene in a leaf-eating monkey. Nat Genet. 2002;30:411-415.
9. Johnson IT, BelshawNJ. Environment, diet and cpg island methylation: epigenetic signals in gastrointestinal neoplasia. Food & Chemical Toxicology An International Journal Published for the British Industrial Biological Research Association. 2008;46(4):0-1359.
10. Wolff GL, Kodell RL, Moore SR, Cooney CA. Maternal epigenetics and methyl supplements affect agouti gene expression in Avy/a mice. Faseb J. 1998;12:949-957.
11. Cooney CA, Dave AA, Wolff GL. Maternal methyl supplements in mice affect epigenetic variation and DNA methylation of offspring. J Nutr. 2002;132:2393S-2400S.

12. Begum G, Stevens A, Smith EB, Connor K, Challis JRG, Bloomfield F, White A.. Epigenetic changes in fetal hypothalamic energy regulating pathways are associated with maternal undernutrition and twinning. Faseb J.2012; 26(4):1694-1703.
13. Liang XF, Liu JK, Huang BY: The role of sense organs in the feeding behaviour of Chinese perch. J Fish Biol. 1998;52:1058-1067.
14. Liang X, Oku H, Ogata H, Liu J, He X. Weaning Chinese perch *Siniperca chuatsi* (Basilewsky) onto artificial diets based upon its specific sensory modality infeeding. Aquac Res. 200;32:76-82.
15. Garcia-Bailo B, Toguri C, Eny KM, El-Sohemy A. Genetic variation in taste and its influence on food selection. OMICS. 2009;13:69-80.
16. Liang XF, Liu JK, Huang BY. The role of sense organs in the feeding behaviour of Chinese perch. J Fish Biol. 1998;52:1058-1067.
17. Irvine JR, Northcote TG. Selection by young rainbow trout (*Salmo gairdneri*) in simulated stream environments for live and dead prey of different sizes. Can J Fish Aquat Sci. 1983;40:1745-1749.
18. Stradmeyer L, Metcalfe NB, Thorpe JE. Effect of food pellet shape and texture on the feeding response of juvenile Atlantic salmon. Aquaculture. 1988;73:217-228.
19. Stradmeyer L. A behavioural method to test feeding responses of fish to pelleted diets. Aquaculture. 1989;79:303–310.
20. Liang XF, Liu JK, Huang BY: The role of sense organs in the feeding behaviour of Chinese perch. J Fish Biol 1998;52:1058-1067.
21. Carlstein, M.. Natural food and artificial, dry starter diets: effects on growth and survival in intensively reared European grayling. Aquaculture International. 1993;1(2):112-123.
22. McEwan IJ, Gustafsson J. Interaction of the human androgen receptor transactivation function with the general transcription factor TFIIF. Proc Natl Acad Sci USA. 1997;94:8485-90.
23. Tan S, Conaway RC, Conaway JW. Dissection of transcription factor TFIIF functional domains required for initiation and elongation. Proc Natl Acad Sci USA. 1995;92:6042-6.
24. Killeen MT, Greenblatt JF. The general transcription factor RAP30 binds to RNA polymerase II and prevents it from binding nonspecifically to DNA. Mol Cell Biol. 1992;12:30-7.
25. Lui JC, Garrison P, Nguyen Q, Ad M, Keembiyehetty C, Chen W, et al. Ezh1 and ezh2 promote skeletal growth by repressing inhibitors of chondrocyte proliferation and hypertrophy. Nature Communications.2016;7:13685.
26. Ai S, Yu X, Li Y, Peng Y, Li C, Yue Y, et al. Divergent requirements for ezh1 in heart development versus regeneration. Circulation Research. 2017; 106-112.
27. Kumar S, Pamulapati H, Tikoo K. Fatty acid induced metabolic memory involves alterations in renal histone h3k36me2 and h3k27me3. Molecular and Cellular Endocrinology. 2015;422:233-242.
28. Yanwei L, Xianlong D, Xuan W, Tingting H, Hao Z, Longshu Y, et al. Genome-wide comparative analysis of dna methylation between soybean cytoplasmic male-sterile line njcms5a and its maintainer njcms5b. Bmc Genomics, 2017;18(1):596.
29. Marcel G, Cornelia D, Huanhuan C, Ilona D, Kerstin S, Sophia S, et al. Comparative dna methylation and gene expression analysis identifies novel genes for structural congenital heart diseases. Cardiovascular Research, 2016;464-477.
30. Mathieu O, Probst AV, Paszkowski J. Distinct regulation of histone h3 methylation at lysines 27 and 9 by cpg methylation in arabidopsis. EMBO J. 2005;24(15):2783-2791.
31. You JJ, Ren P, He S, Liang XF, Zhang YP. Histone methylation of h3k4 involved in the anorexia of carnivorous mandarin fish (*siniperca chuatsi*) after feeding on a carbohydrate-rich diet. Front Endocrinol. 2020;11.
32. Wang L, Feng Z, Wang X, Wang X, Zhang X. DEGseq, an R package for identifying differentially expressed genes from RNA-seq data. Bioinformatics. 2010;26(1):136-138.
33. Huang JF, Shen ZY, Mao QL, Zhang XM, Zhang B, Wu JS, et al. Systematic analysis of bottlenecks in a multibranched and multilevel regulated pathway: the molecular fundamentals of l-methionine biosynthesis in *Escherichia coli*. ACS Synth Biol.2018;7.
34. Zhou LF, Zhao BW, Guan NN, et al. Plasma metabolomics profiling for fish maturation in blunt snout bream. Metabolomics. 2017;13(4):40.
35. Vandesompele J, Preter KD, Pattyn F, Poppe B, Roy NV, Paepe AD. Accurate normalization of real-time quantitative RT-PCR data by geometric averaging of multiple internal control genes. Genome Biol. 2018;3:1-12.
36. Liang H, He S, Liang XF, Lu HL,Chen K. Feeding habit transition induced by social learning through CAMKII signaling in chinese perch (*siniperca chuatsi*). Aquaculture, 2020;533.
37. Livak KJ, Schmittgen TD. Analysis of relative gene expression data using real-time quantitative PCR and the 2−ΔΔCT method. Methods. 2001;**25**:402-408.
38. Cai WJ, He S, Liang XF, Yuan XC. DNA methylation of T1R1 gene in the vegetarian adaptation of grass carp *ctenopharyngodon idella*. Scientific reports, 2018;8:6934.

Figures

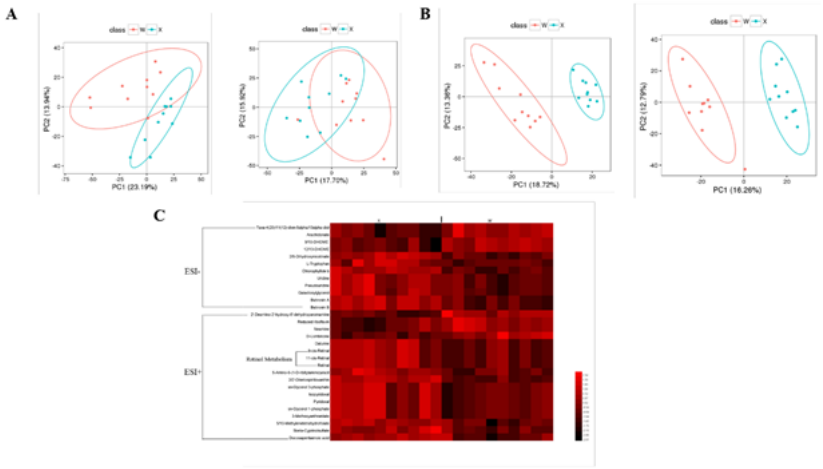

Figure 2

A. PCA scores scatter plot in positive ion (left) and in negative ion (right) scan modes for the two groups. B. PLS-DA scores scatter plot in positive ion (left) and in negative ion (right) scan modes for the two groups. C. The heat map of differential metabolites from the related pathways between the two groups in both positive and negative mode. Each line represents a differential metabolite and each cross represents a plasma sample group. Different colors represent different abundance intensity, and the higher abundance intensity shows a gradual increase from dark color to red color.

Supplementary Files

This is a list of supplementary files associated with this preprint. Click to download.

- supplementaryfile.docx